Feasibility of using radar differential Doppler velocity and dual-frequency ratio for sizing particles in thick ice clouds

Sergey Y. Matrosov[1]

Received 25 February 2011; revised 6 July 2011; accepted 13 July 2011; published 8 September 2011.

[1] Measurements from ground-based collocated K_a- and W-band vertically pointing Doppler radars were used to evaluate the differential Doppler velocity (DDV) approach for retrieving a size parameter of the aggregate particle distributions in ice clouds. This approach was compared to a more traditional method based on the dual-frequency reflectivity ratio (DFR) using case study observations in different clouds. Because of measurement errors and other uncertainties, meaningful DDV-based retrievals were generally available for the size slope parameter interval of 9 $cm^{-1} < \Lambda < 25$ cm^{-1}. The DFR were generally available for particle populations with Λ up to about 45 cm^{-1}. Expected retrieval errors in the Λ interval between 9 cm^{-1} and 25 cm^{-1} were about 40% for the DFR-based estimates and about a factor of 2 larger for the DDV method. Errors increase for noisier measurements. Comparisons of the DDV- and DFR- inferred values of Λ when both retrievals were available revealed their general consistency with a relative standard deviation between results being within retrieval uncertainties. While the DFR approach appears to be more accurate, it requires a 0 dB constraint near cloud tops, which mitigates uncertainties in absolute radar calibrations and differing attenuation paths. The DDV approach generally does not require such a constraint if radar beams are perfectly aligned in vertical (which might not be exactly a case during some observations). Given this, DDV measurements may potentially allow ice particle sizing in situations when DFR constraining is not effective or available (e.g., in precipitating clouds and in clouds with substantial amounts of supercooled water).

Citation: Matrosov, S. Y. (2011), Feasibility of using radar differential Doppler velocity and dual-frequency ratio for sizing particles in thick ice clouds, *J. Geophys. Res.*, *116*, D17202, doi:10.1029/2011JD015857.

1. Introduction

[2] Ice clouds of the upper troposphere cover a significant fraction of the globe. They modulate the incoming solar radiation and outgoing long-wave radiation. Improving parameterizations of cloud feedbacks remains an important issue for climate models. The main microphysical properties of ice clouds that determine their radiation impact in models are ice water content (IWC) and size of ice particles, which characterizes the whole distribution (e.g., effective, mean, or median size). A number of remote sensing techniques have been suggested for retrievals of ice cloud microphysical parameters using ground-based instruments [*Comstock et al.*, 2007].

[3] Cloud particle characteristic size is one of the parameters which is usually retrieved by the radar-infrared (IR) radiometer approaches [e.g., *Matrosov et al.*, 1992; *Mace et al.*, 1998], radar-lidar approaches [e.g., *Donovan and van Lammeren*, 2001; *Wang and Sassen*, 2002; *Okamoto et al.*, 2003], and the single Doppler radar approaches [e.g., *Matrosov et al.*, 2002; *Mace et al.*, 2002]. Retrievals of characteristic size that utilize optical instruments such as IR radiometers or lidars are applicable only to relatively thin ice clouds that are unobstructed by liquid layers as observed from the ground. Single-frequency Doppler radar methods rely on mean vertical Doppler velocity measurements to infer characteristic particle size. These measurements are affected by vertical air motions. Even though special procedures are usually applied to mitigate vertical air motion contributions (e.g., time averaging of Doppler measurements), they contribute noticeably retrieval uncertainties. Long time averaging also results in a loss of details in cloud structure estimates. Independent estimates of cloud particle characteristic size are often desirable.

[4] It has been demonstrated that dual-frequency radar measurements can be used to estimate characteristic particle sizes in ice clouds when scattering for at least one of the radar wavelengths is sufficiently outside the Rayleigh regime [e.g., *Matrosov*, 1993; *Sekelsky et al.*, 1999; *Hogan et al.*, 2000; *Wang et al.*, 2005; *Liao et al.*, 2008]. The interest in

[1]Cooperative Institute for Research in Environmental Sciences, University of Colorado at Boulder, and Earth System Research Laboratory, NOAA, Boulder, Colorado, USA.

0148-0227/11/2011JD015857

dual-frequency radar-based particle size retrievals is, in part, instigated by the availability of dual-frequency cloud radars operating at W-band (wavelength, $\lambda \sim 3$ mm) and K_a-band ($\lambda \sim 8$ mm) frequencies. Such radars will be permanently deployed at different Atmospheric Radiation Measurement (ARM) Climate Research Facilities (ACRFs) operated by the U.S. Department of Energy.

[5] The requirement for scattering being sufficiently outside the Rayleigh regime naturally limits applications of dual-frequency radar approaches to clouds containing relatively large particles. For the W- and K_a-band pair, reflectivity differences exceed ~1 dB for spherical particle populations with median volume sizes, D_0, which are greater than several hundred microns [*Matrosov*, 1993; *Hogan et al.*, 2000]. Particles with such sizes, however, are not uncommon even in clouds that do not produce precipitation reaching the ground [*Mazin*, 1989]. Such particles are also observed in snowfall and precipitating ice clouds producing rainfall as a result of melting.

[6] Most dual-frequency radar retrievals of characteristic particle sizes in ice clouds are based on measurements of the dual-frequency ratio (DFR) of reflectivity factors at two frequencies. The vertical (or nadir) looking Doppler radars, however, provide another way to get size estimates. The difference between vertical Doppler velocities at two radar frequencies, which is sometimes referred to as differential Doppler velocity (DDV), also depends on particle characteristic size. Unlike single-frequency Doppler measurements, DDV is not affected by vertical air motions because their contributions are the same at both frequencies, and these contributions cancel out each other when calculating DDV.

[7] DDV measurements with airborne nadir-looking W- and X-band ($\lambda \sim 3$ cm) radars have been used for estimating characteristic drop size in rainfall [e.g., *Tian et al.*, 2007]. *Liao et al.* [2008] also used DDV from these radars for snow retrievals. They concluded that the necessary precision is difficult to achieve from airborne data due to aircraft vibrations and pointing errors. The ground-based measurements, however, are more stable, and DDV estimates from such measurements may be more useful for inferring characteristic size of ice particles (or snowflakes). The main objective of this study is to evaluate feasibilities and estimate potential errors for ground-based radar retrievals of size parameters in ice clouds using W- and K_a-band radar measurements of DDV and compare them to more traditional DFR-based retrievals. This has an implication for future dual-frequency radar measurements at different ACRFs.

2. Dual-Frequency Radar Parameters

[8] The dual-frequency radar ratio for the ARM cloud radar frequencies is defined as

$$\mathrm{DFR} = 10\ \log_{10}[\mathrm{Z_e(K_a)}/\mathrm{Z_e(W)}]. \quad (1)$$

[9] In (1) the effective radar reflectivity factors, Z_e (hereafter reflectivities), are given as [*Doviak and Zrnic*, 1993]

$$Z_e(\lambda) = \lambda^4\pi^{-5}\left|\left(m^2+2\right)/\left(m^2-1\right)\right|^2 \int \sigma_b(D,\lambda)N(D)dD, \quad (2)$$

where $N(D)$ is the particle size distribution (PSD), $\sigma_b(D, \lambda)$ is the backscatter cross section, and m is the complex refractive index of water. The integration is performed with respect to the particle size D expressed in terms of the major particle dimension from 10 μm to 3 cm.

[10] Typically, size distributions of atmospheric hydrometeors are approximated by the gamma function [*Mazin*, 1989]:

$$N(D) = N_o\ D^{\mu} \exp[-(3.67+\mu)D/D_0], \quad (3)$$

where N_o is the scaling factor, μ is the distribution shape factor, and D_0 is the median volume particle size. While, according to *Mazin* [1989], μ is generally between 0 and 2 in different ice clouds, different parameterizations often use the exponential distribution ($\mu = 0$) with the size parameter Λ:

$$N(D) = N_o \exp(-\Lambda D), (\text{where } \Lambda \approx 3.67/D_0). \quad (4)$$

[11] Of particular interest for this study are thick ice clouds that produce measurable dual-frequency signals. In these clouds and snowfall, PSD moments are dominated by larger particles which often are aggregates. It was shown by *Heymsfield et al.* [2008] that for clouds with the Rayleigh approximation reflectivity $Z_e > 5$ dBZ and size slope parameter $\Lambda < 40$ cm^{-1}, the analytical representations of experimental PSDs with more variables than exponentials (e.g., gamma-function PSD) are not required to accurately derive size distribution moments including radar reflectivity and ice content. Given that, the exponential PSD was therefore assumed. The slope Λ defines the particle size (e.g., D_0) characterizing the whole distribution. It will be used as a size parameter further in this study. Considering Λ as a substitute for the PSD characteristic size is also justified because the slope parameter is widely used in different experimental studies on cloud microphysics [e.g., *Heymsfield et al.*, 2008]. While the exponential distribution is further assumed, the uncertainty associated with this assumption is estimated in section 3.

[12] For vertically pointing radars, the measured Doppler velocity, V_D, is given by [e.g., *Doviak and Zrnic*, 1993]

$$V_D(\lambda) = \lambda^4\pi^{-5}\left|\left(m^2+2\right)/\left(m^2-1\right)\right|^2 Z_e^{-1}(\lambda) \cdot \int \sigma_b(D,\lambda)V_t(D)N(D)dD + w_a, \quad (5)$$

where $V_t(D)$ is the particle terminal fall velocity and w_a is the vertical air motion. Note that turbulence broadening effects do not affect V_D, so they were neglected here. For the cloud radar pair operating at K_a- and W-bands, differential Doppler velocity is given by the difference

$$\mathrm{DDV} = V_D(\mathrm{K_a}) - V_D(\mathrm{W}). \quad (6)$$

[13] Both DFR and DDV do not depend on the PSD scaling parameter N_o. The fact that the DDV does not depend on vertical air motions can make this parameter an alternative to the single-frequency vertical Doppler velocity, which is also sometimes used for particle sizing. For single-frequency measurements a generally unknown contribution of w_a increases estimation uncertainties and a significant time averaging is usually required to reduce these

uncertainties. Long time averaging effectively reduces the time resolution of retrievals.

3. Simulations of Observational Parameters DFR and DDV

[14] In order to assess retrieval potentials, the Λ-DFR and Λ-DDV relations and their variability need to be estimated. These relations are determined by $\sigma_b(D, \lambda)$ and $N(D)$. There is an additional influence of the V_t-D relation on DDV. Unlike for water drops, there is some significant variability in the V_t-D relation for ice particles and snowflakes. For different aggregate particles *Lumb* [1961] suggested the power law relations,

$$V_t\left(\mathrm{m\,s^{-1}}\right) = aD(\mathrm{mm})^b, \tag{7}$$

where $b = 0.25$ and the coefficient a generally varies from about 0.55 to 0.85 for normal atmospheric pressure ($P \approx$ 1013 hPa).

[15] Figure 1 shows particle terminal velocities as a function of size for the mean value of $a = 0.7$, as well as for $a = 0.55$ and $a = 0.85$. Also shown is the V_t–D relation used by *Matrosov* [2007]. This relation approximates the ice aggregate data presented by *Mitchell and Heymsfield* [2005], and it corresponds to the mean Lumb relation (i.e., $V_t = 0.7D^{0.25}$) relatively well. Lumb's relations are also in good agreement with experimental data from *Brandes et al.* [2008] who provide values of a in the range between 0.55 and 0.87 with exponent b being around 0.23–0.25.

[16] Further, in this study, it is assumed that $b = 0.25$ and the mean value of the coefficient a is 0.70. A 20% uncertainty of this coefficient approximately corresponds to the fall velocity bounds shown in Figure 1 by relations $V_t = 0.55D^{0.25}$ and $V_t = 0.85D^{0.25}$. The fall velocities at altitude h above mean sea level (MSL) need to be increased using the factor s, which depends on pressure P [*Pruppacher and Klett*, 1978]:

$$s = [1013/P(h)]^{0.45}. \tag{8}$$

[17] The correspondence between the backscatter cross section σ_b and particle size D for the most part determines Λ-DFR relations and influences Λ-DDV relations. For a given particle size, these cross sections depend on particle density, shape, and orientation. Particle bulk density affects individual values of σ_b rather strongly. The density effects on DFR and DDV values, however, are generally insignificant, as will be shown later in this section.

[18] The simplest shape model for aggregate ice particles is a spherical model. It has been shown that this model may not be appropriate for calculating backscatter at higher radar frequencies, especially for vertical (or nadir) viewing [e.g., *Matrosov et al.*, 2005a]. Experimental data [e.g., *Korolev and Isaac*, 2003] indicate that ice aggregates typically have aspect ratios, r, of about 0.6–0.8, and these ratios do not significantly depend on particle size. Comparisons of model calculations and experimental observations showed that the oblate spheroidal particle model implying such ratios satisfactorily describes observed DFR values measured with an airborne nadir-pointing radar [*Matrosov et al.*, 2005a]. The spheroidal model is a relatively simple way to describe generally nonspherical particles. This model has been used by the radar meteorology community previously [e.g., *Doviak and Zrnic*, 1993], including dual-frequency radar studies of hydrometeors [e.g., *Matrosov et al.*, 2005a], and was shown to satisfactorily describe radar properties of particles in high-reflectivity ice clouds by *Reinking et al.* [2002], who presented experimental evidence that this model provided well-described radar measurements including polarimetric parameters, which are shape model sensitive. This model was used in this study.

[19] The backscatter cross sections were calculated using the T-matrix method [*Barber and Yeh*, 1975]. This method proved to be useful for modeling radar properties of different nonspherical hydrometeors at radar frequencies. It was further assumed that due to aerodynamic forcing, ice particles are oriented preferably with their major dimensions in the horizontal plane, and the standard deviation from this preferred orientation is 9°. In the absence of strong electrical fields and wind shear, such preferred orientation of nonspherical ice particles was inferred from dual-polarimetric scanning radar measurements [*Matrosov et al.*, 2005b].

[20] Simulations of observational parameters DFR and DDV as a function of Λ using different assumptions are shown in Figure 2 for the K_a- and W-band pair corresponding to wavelengths of 8.7 and 3.2 mm. Note that the attenuation of the radar signals is ignored in simulations. This attenuation is irrelevant for DDV measurements. While it is affecting DFR measurements, the differential attenuation effects in the lower atmospheric layers can be largely removed by constraining the DFR at 0 dB near ice cloud tops, as will be shown in section 4. Figure 2a shows Λ-DFR and Λ-DDV relations calculated for assumptions of typical particle aspect ratios, r, of 0.6 and 0.8. The data presented in Figure 2a correspond to simulations for the exponential PSD and the particle mass; size relations as prescribed by *Brown and Francis* [1995]. It can be seen that particles with a greater degree of nonsphericity (i.e., with smaller values of r) generally produce weaker dual-frequency effects [*Matrosov et al.*, 2005a]. As characteristic particle sizes decrease and the slope Λ increases, both DFR and DDV approach zero, as Rayleigh scattering dominates radar signals. Note that for simplicity when calculating relations shown in Figure 2, the factor $|(m^2+2)/(m^2-1)|^{-2}$ in (1) was set to 0.9 for both frequencies. This does not affect the shape of the Λ-DFR curves. Changes in the water refractive index m at K_a- and W-frequencies, which result in the differences in this constant factor, would only shift this curve. A DFR limit of 0 dB for very large values of Λ (i.e., for small particle populations) adds convenience when interpreting measurement data without losing generality.

[21] Figure 2b shows influence of the PSD shape. Simulations are presented for the exponential distribution ($\mu = 0$) and the second-order gamma-function PSD ($\mu = 2$). A scaled exponential slope for the gamma-function PSD is depicted: $\Lambda(\mu) = 3.67(3.67 + \mu)^{-1}\,\Lambda(\mu = 0)$. For this slope, the gamma-function PSD corresponds to the same median volume particle size D_0 as the exponential PSD. Comparing Figures 2a and 2b indicates that the DFR and DDV variability due to expected particle shape (i.e., aspect ratio) changes is noticeably greater than that due to PSD shape changes. It is evident from data in Figures 2a and 2b that

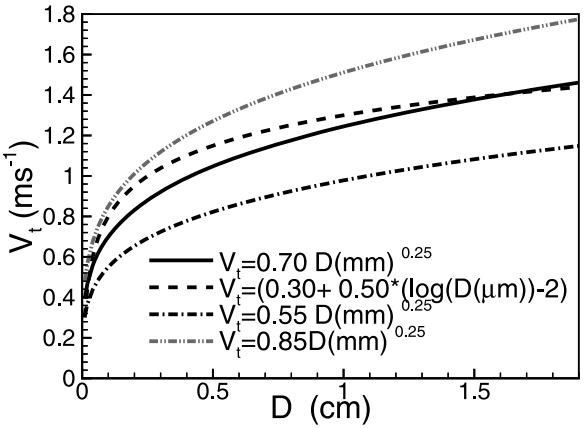

Figure 1. Terminal velocity of ice particle aggregates as a function of hydrometer size.

DFR and DDV absolute variability due to PSD changes is typically within 30% of changes due to expected particle aspect ratio variability. Assuming that uncertainties due to these two factors are uncorrelated (i.e., the total uncertainty is the square root of the sum of individual uncertainties squared), it can be estimated that the total combined uncertainty due to changes in particle aspect ratio between $r = 0.8$ and $r = 0.6$ and due to PSD changes between $\mu = 0$ and $\mu = 2$ increases only by less than 10% compared to the uncertainty solely due to aspect ratio changes. Given this estimate, it was further assumed that the PSD-caused uncertainties in the DFR-Λ and DDV-Λ relations can be neglected compared to the uncertainties due to particle shape changes. Such an assumption is further justified in light of findings by *Heymsfield et al.* [2008] who indicated that the exponential function satisfactorily describes experimental PSDs for high-reflectivity ice clouds.

[22] The choice of the particle mass-size relation (i.e., density) influences the DFR-Λ and DDV-Λ relations relatively little. This can be seen in Figure 2c where simulations are presented for the assumption of the *Brown and Francis* [1995] mass and for the case when that mass (and hence particle density) was increased by a factor of 2. While there is not much change in the DFR-Λ relations for these two mass assumptions, the DDV-Λ dependence shows some modest variability. This variability is, however, significantly smaller than that due to the particle shape uncertainty. The corresponding contribution to the total model uncertainty is expected to be even less than that due to the aforementioned changes in μ (if the independence of the error contribution is assumed) and was neglected.

4. Case Studies of Dual-Frequency Radar Measurements and Retrievals

[23] The deployment of new ARM polarimetric cloud radars operating at W- and K_a-band frequencies at different ACRFs is expected in near future. Testing the DFR and DDV approaches for estimating Λ, however, now can be performed with existing data. For some period of time, the ARM 8.7 mm wavelength Cloud Radar (MMCR) and the 3.2 mm W-band ARM Cloud Radar (WACR) were simultaneously operated at the Southern Great Plains (SGP) ACRF. The WACR has a ~0.35° beam width and a 43 m vertical resolution. It has one mode of operation. The beam width of MMCR is 0.2° and it cycles through several operation modes that are optimized for specific types of

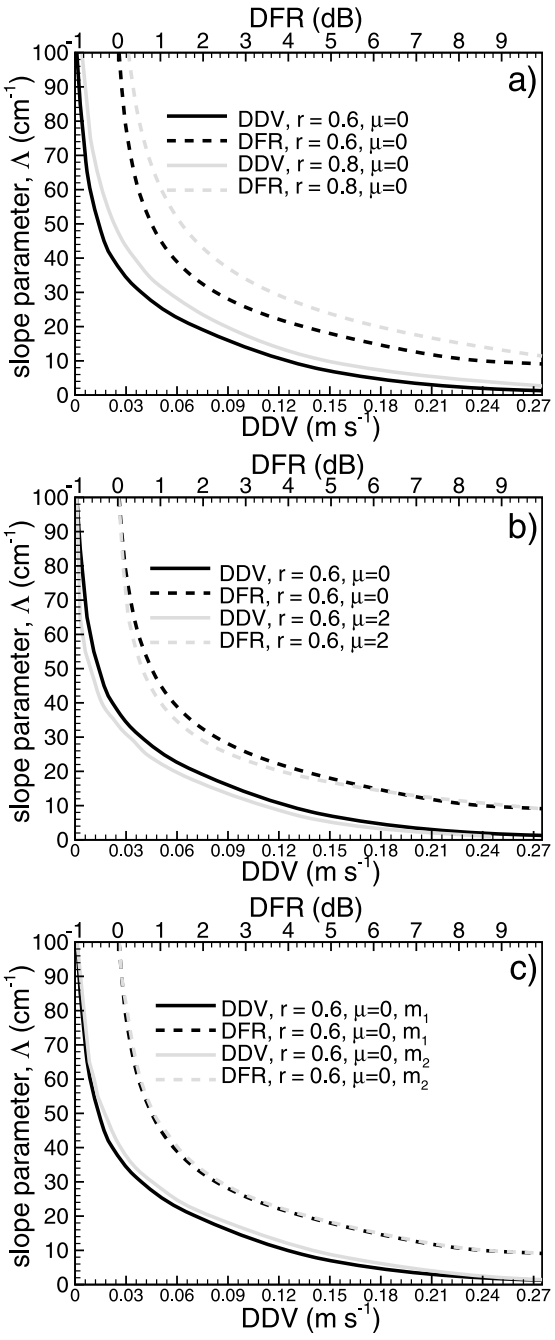

Figure 2. Slope parameter Λ as a function of W- and K_a-band differential Doppler velocity (DDV, lower x axis) and dual-frequency ratio (DFR, upper x axis) for (a) two assumptions for particle aspect ratios $r = 0.6$ and $r = 0.8$, (b) two assumptions of the order of the gamma-function size distribution $\mu = 0$ and $\mu = 2$, and (c) two assumptions about particle-size mass relation. The *Brown and Francis* [1995] mass-size relation was assumed, except for the data shown by gray lines in Figure 2c, where mass was increased by a factor of 2 compared to this relation.

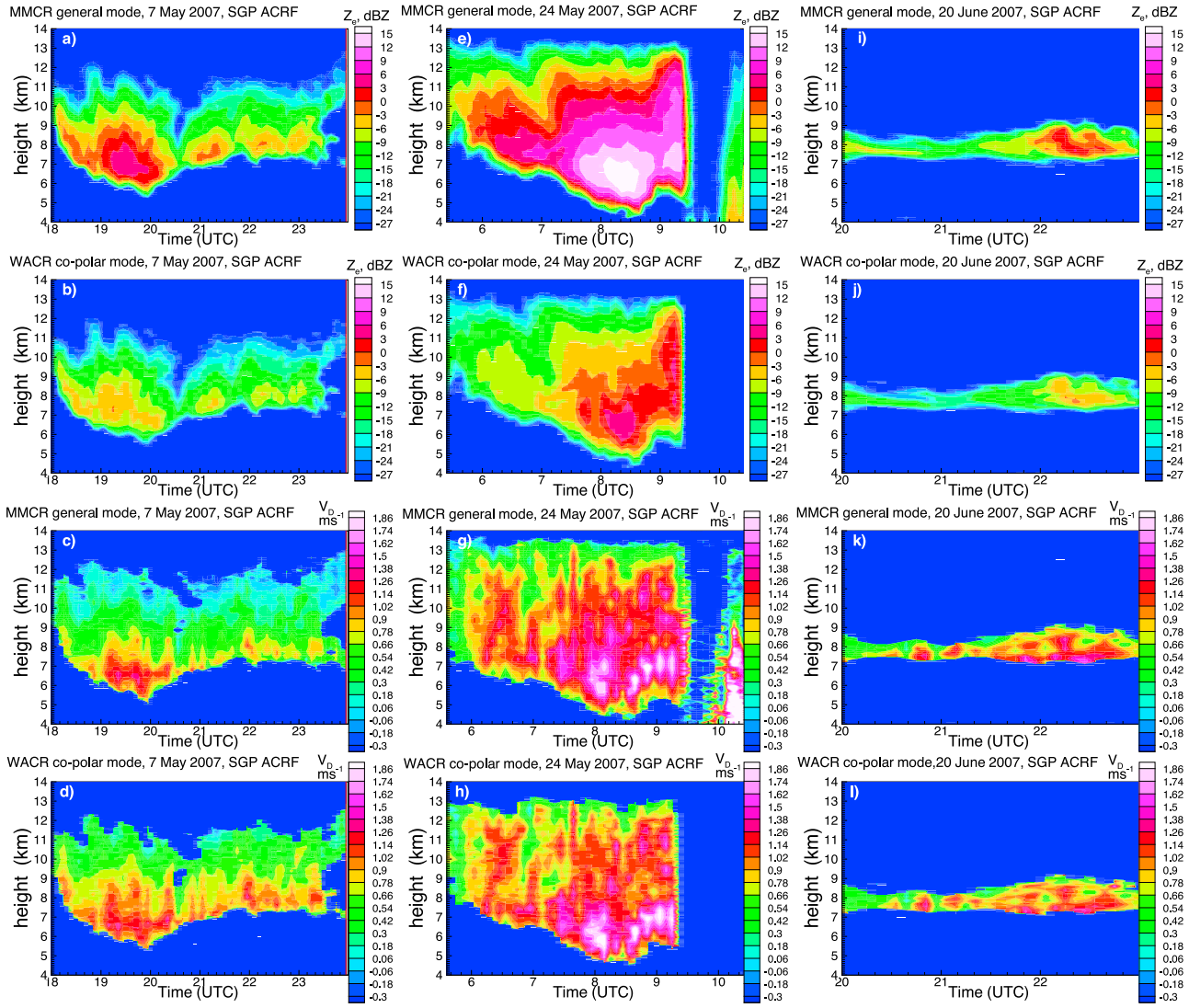

Figure 3. (a, c, e, g, i, k) K_a-band millimeter wavelength cloud radar (MMCR) and (b, d, f, h, j, l) W-band ARM cloud radar (WACR) measurements of reflectivity (Figures 3a, 3b, 3e, 3f, 3i, 3j) and vertical Doppler velocity (Figures 3c, 3d, 3g, 3h, 3k, 3l) during observations of isolated ice clouds on 7 May and 20 June 2007 and an anvil on 24 May 2007.

hydrometeors. Measurements in the general operation mode, which has a vertical resolution of 90 m, are the most robust, and they are the ones used here. The WACR data were interpolated and averaged to the common with MMCR vertical grid of 90 m resolution.

4.1. K_a- and W-Band Radar Measurements in Ice Clouds

[24] Figure 3 shows time-height cross sections of reflectivity and Doppler velocity measurements from the vertically pointing MMCR and WACR during several hour long observations of isolated ice clouds in the upper troposphere on 7 May and 20 June 2007, and of an anvil ice cloud on 24 May 2007. While the clouds observed on 7 May and 20 June 2007 did not produce precipitation at the ground, the anvil observed on 24 May 2007 was part of a convective system that produced heavy rainfall at the radar site after about 09:20 UTC. This rainfall totally attenuated radar signals. No significant radar echo, however, was present between the anvil and the ground prior to 09:10 UTC, so a period before this time was of interest. Bases for clouds of interest in Figure 3 were higher than about 4.5 km, which was well above the freezing level located at a height of about 2.7–3 km for all cases as independent measurements indicated [*Matrosov*, 2009]. The radar data were gridded to the same vertical resolution of 90 m. Measurements were averaged in 6 min intervals to mitigate the radar beam width difference. It was suggested [*Hogan et al.*, 2005] that temporal averaging for vertically pointing radar measurements alleviates cloud inhomogeneity effects on dual-frequency parameters when beam widths are not exactly matched.

[25] Microwave radiometer (MWR) measurements (not shown) indicated that the columnar amount of the atmospheric water vapor during the 7 May 2007 cloud observations varied in a range between 31 and 34 mm. The radiometer-derived liquid water path (LWP) values were generally within the

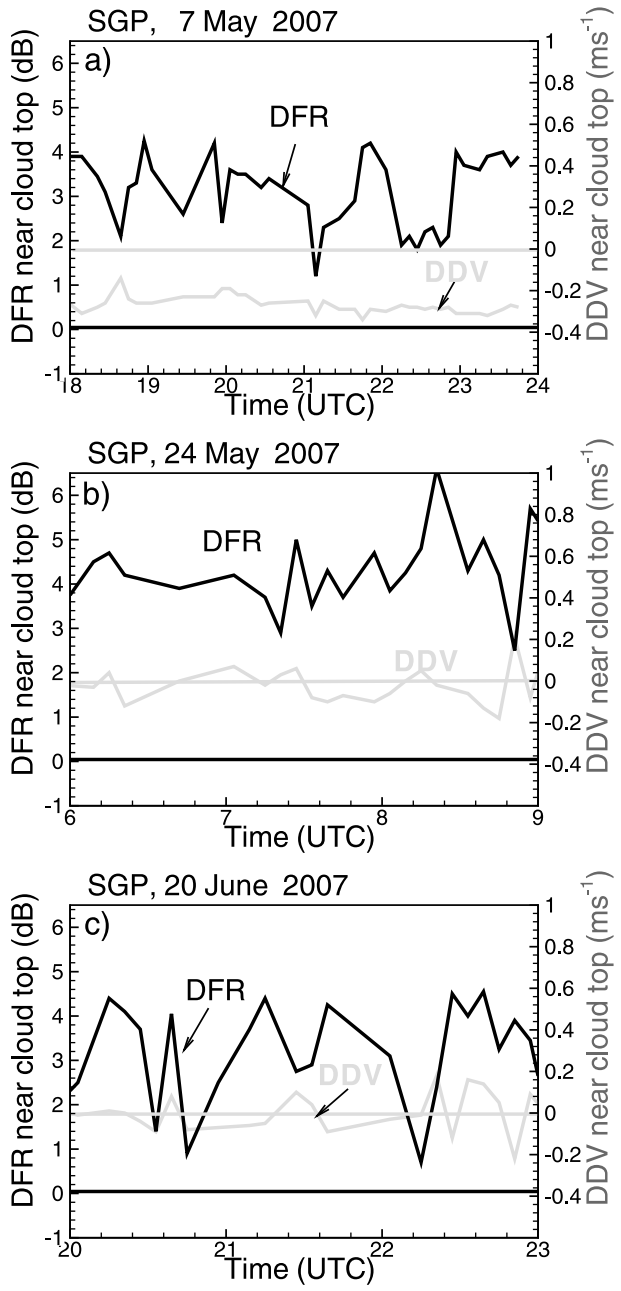

Figure 4. Time series of DFR and DDV measurements near the cloud top (Ze ~ −26 dBZ) for the (a) 7 May 2007, (b) 24 May 2007, and (c) 20 June 2007 observational cases. Horizontal lines show DFR = 0 dB (black) and DDV = 0 ms^{-1} (gray).

measurement noise except for the period between 20:10 and 22:00 UTC, when some thin boundary layer clouds were present at lower altitudes. This suggests that the amount of supercooled liquid (if any) in the observed ice cloud was negligible. Note that the intermittent presence of the thin boundary layer clouds did not cause any significant changes/trends in DFR near cloud tops as shown later in this section. For the anvil cloud on 24 May 2007, the MWR measurements indicated about 36–37 mm of atmospheric water vapor and LWP values of about 70–75 g m^{-2} (not shown). This relatively steady amount of LWP if contained in tenuous boundary layer clouds does not significantly affect dual-wavelength radar retrievals if the reflectivity measurement constrain is made at the cloud top. Moreover, even if this amount is present as supercooled water in the upper ice cloud, the resulting total differential attenuation will be only a few tenths of 1 dB, which is less than DFR measurement uncertainty. LWP values for the event of 20 June 2007 associated with low-altitude boundary layer clouds were more variable than for two other cases. They were generally between 30 and 80 g m^{-2}. These modest LWP changes may have resulted in somewhat higher variability of DFR estimates at the cloud top compared to the other two cases.

[26] Both radars similarly detected cloud boundaries. The K_a-band reflectivity values are noticeably greater than those at W-band, especially in lower cloud parts where larger particles usually reside and stronger non-Rayleigh scattering effects are expected at the higher radar frequency. The K_a-band vertical Doppler velocities are generally greater than those at W-band for the anvil cloud; however, they are quite similar for the 7 May 2007 case, which is somewhat counterintuitive, because generally lower V_D values at W-band are expected for larger hydrometeors. To clarify this discrepancy, the time series of radar measurements in the vicinity of cloud tops was analyzed.

[27] The time series of DFR and DDV values from the highest range gate where reflectivity data from both the MMCR and the WACR were well above (by ~10 dB or so) the receiver noise levels are plotted in Figure 4. It was made sure that for the period of averaging this gate level is below the absolute highest radar gates where possible beam filling effects are usually the strongest. The corresponding reflectivities, which came from regions near radar cloud tops, were around −26 dBZ for the MMCR (and similar for the WACR). Cloudy regions near cloud top levels that exhibit such low reflectivities typically consist of small particles, which are in the Rayleigh scattering regime for both frequencies. Given that, one could expect that both DFR and DDV there should be around zero.

[28] The mean value of the observed DFR for the 7 May 2007 cloud is 3.1 dB, and the standard deviation (SD) around this mean value is about 0.9 dB. For the anvil cloud on 24 May and the 20 June cloud, these values are about 4.3 and 0.9 dB, and 2.6 and 1.2 dB, correspondingly. The higher SD value for the 20 June cloud may be due in part to larger variability in low-level cloud LWP for this event. There are a number of reasons why MMCR and WACR reflectivities are a little different at the cloud top. One reason is different total attenuations of the atmosphere at K_a- and W-band frequencies. Possible calibration errors (and different values of frequency-dependent water refractive indices used for calibrations) of the radars can also be responsible. For the purpose of this study, however, the exact reason for the mean difference is not important. The DFR bias corrections could be introduced in the measurements of these two clouds to make DFR observations consistent.

[29] There are no obvious trends in the DFR measurements with time at the cloud top for a given cloud. A DFR SD value of ~0.9 dB at the cloud top heights could be considered here as the uncertainty of the DFR measurements. Part of this uncertainty is likely due to the temporal variability of atmospheric transmittance, which is different

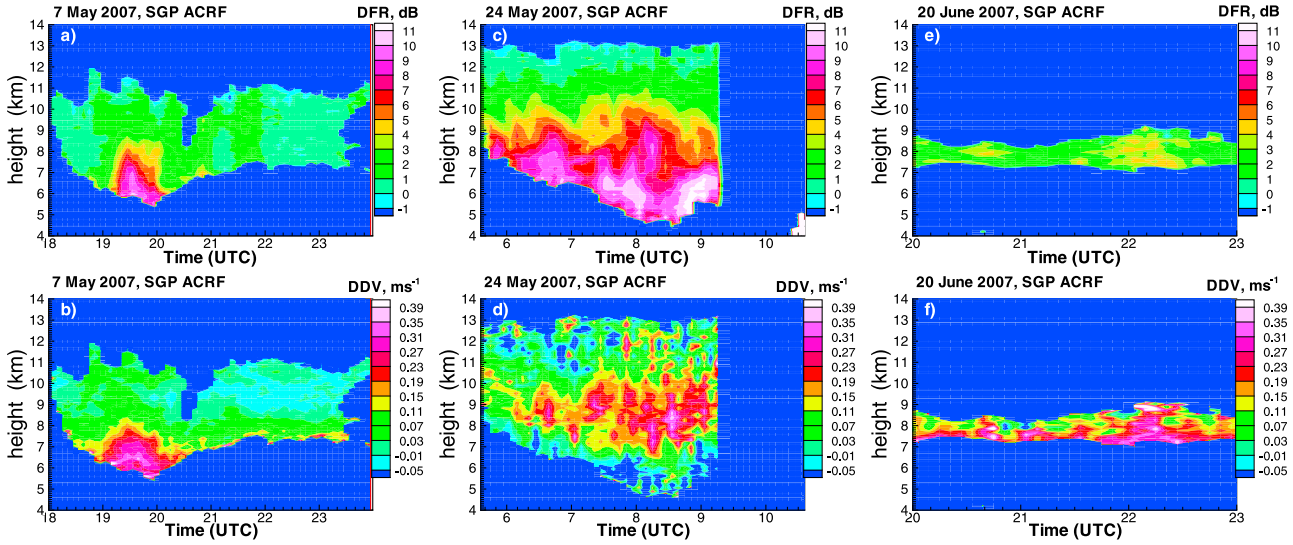

Figure 5. Time-height cross sections of (a, c, e) DFR and (b, d, f) DDV measurements after correcting biases for the observational cases of 7 May 2007 (Figures 5a and 5b), 24 May 2007 (Figures 5c and 5d), and 20 June 2007 (Figures 5e and 5f).

for K_a- and W-band frequencies. Other reasons for this uncertainty are the fluctuating nature of measured signals [e.g., *Marshall and Hitschfeld*, 1953] and effects due to differing beam widths and range resolutions.

[30] The mean DDV biases near the top of the clouds observed on 24 May and 20 June 2007 are about zero, and the corresponding DDV SD values are about 0.06 m s^{-1}. The mean value of the DDV bias for the ice cloud observed on 7 May 2007, however, is −0.27 m s^{-1}, and the corresponding standard deviation is about 0.03 m s^{-1}. Since Doppler measurements are not affected by the radar absolute calibration and signal attenuation, one likely reason for the DDV bias is radar pointing error for this particular observation time (although other reasons cannot be disregarded). If one or both radars were not pointing exactly at zenith, the horizontal wind component could "leak" in DDV estimates. Some pointing errors could occur during radar deployment and can change in time. Note that other researchers also observed MMCR-WACR Doppler velocity discrepancies (e.g., G. G. Mace, private communication, 2010). As with the DFR for a given cloud, the DDV bias can be effectively removed without significantly compromising the subsequent retrievals of the slope parameter. The DDV standard deviation value could be considered as an uncertainty of bias-corrected DDV measurements. Similar to the DFR, there is no significant trend with time for DDV measurements near the cloud top for the considered observational cases.

[31] Bias-corrected DFR and DDV measurements for all three observational cases are shown in Figure 5. Differential attenuation effects inside the clouds due to absorption in atmospheric gases (oxygen and water vapor) were accounted for in the DFR data through modeling using the ARM merged radiosonde sounding information on temperature, atmospheric pressure, and humidity. The differential attenuation effects due to ice attenuation were accounted for using relations between the attenuation coefficient and reflectivity estimated from the results of the modeling study presented by *Matrosov* [2007].

[32] For the cloud observed on 7 May 2007, the DDV bias of −0.27 m s^{-1} was estimated near the cloud top height. It was assumed that the bias remains the same below this height, though uncertainties associated with this assumption are evaluated in section 4.2. Some justification for this assumption can be found in the fact that the horizontal winds, which contribute to vertical Doppler measurements for tilted beams, did not exhibit significant variability inside the cloud during observations, so their contribution does not change very significantly. Horizontal wind directions and speeds as given in the ARM merged sounding product are shown in Figure 6. It can be seen from Figure 6 that a general horizontal flow was not changing drastically in the observed cloud.

[33] It can be seen from Figure 5 that more measurement noise is present in differential Doppler velocity data compared to DFR estimates. This noise is especially evident in the uppermost part ($h > 11$ km) and the lowest part ($h < 7$ km) of the anvil cloud (24 May 2007), where the DDV values are unexpectedly low. Note that the DDV SD values for this event at the cloud top were also higher than for the cloud observed on 7 May 2007. Possible reasons for DDV noisiness in the lower part of this cloud, where DFR data indicate the largest particles, are discussed in section 4.2.

4.2. Dual-Frequency Retrievals of PSD Slope Λ

[34] Results of retrievals of the exponential PSD slope parameter Λ for all ice cloud observational cases are shown in Figure 7. Retrievals were performed using the bias-corrected DFR and DDV measurements shown in Figure 5 and the Λ-DFR and Λ-DDV relations from Figure 2 assuming the particle aspect ratio of 0.6. This aspect ratio was found to best explain the airborne dual-frequency measurements at X- and W-band radar pair [*Matrosov et al.*, 2005a] and to be representative for a large set of microphysical measurements [*Korolev and Isaac*, 2003]. DDV data used for retrievals were adjusted for changing with height pressure using (8).

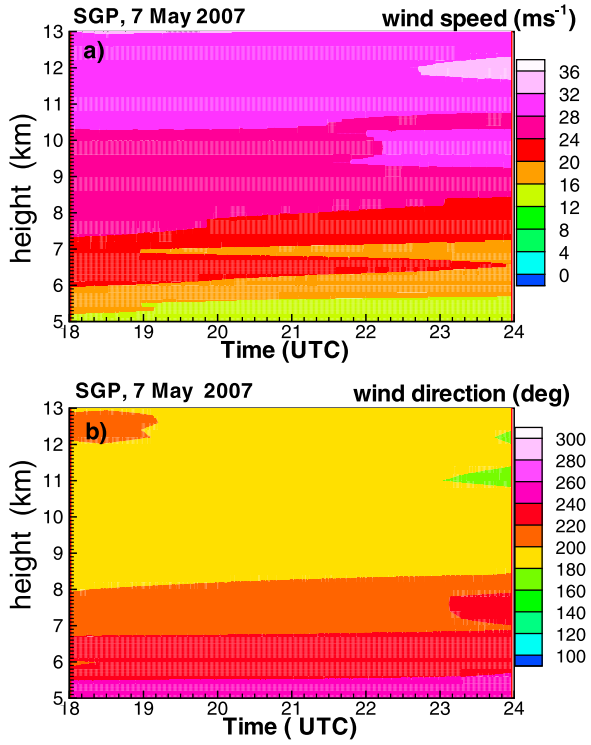

Figure 6. Time-height cross section of (a) horizontal wind speeds and (b) directions as inferred from ARM merged soundings for the observational case of 7 May 2007.

[35] As seen from Figure 2, the DFR and DDV values, which are close to their uncertainties (i.e., ~0.9 dB and ~0.03 m s^{-1}) estimated as the SDs of these parameters near the cloud top for the case of 7 May 2007, correspond to Λ values of about 45 cm^{-1} and 35 cm^{-1}, respectively. This indicates that Λ values that exceed 45 cm^{-1} (or 35 cm^{-1}) most likely cannot be retrieved from measurements of DFR (or DDV) with reasonable accuracy, so retrievals for the cloud regions with DFR less than 0.9 dB and DDV less than 0.03 m s^{-1} are not shown. The cloud top DDV SDs for cloud cases of 24 May and 20 June 2007 were larger than for the 7 May 2007 event. Λ values that are larger than about 25 cm^{-1} correspond to DDV values that are less than about 0.06 m s^{-1} and may be not reliable for these clouds given the higher DDV SDs for these cases. The corresponding noisy retrievals are generally seen in the upper parts of the 24 May and 20 June 2007 clouds.

[36] The best agreement between DFR- and DDV-based retrievals is seen in the lower part of the 7 May 2007 cloud (i.e., between 5.5 and 8 km in the 19:00–20:30 UTC time interval), in the middle of the anvil cloud of 24 May 2007 in Figure 7b (i.e., between about 7 and 10 km), and in parts of the 20 June 2007 cloud. The DFR- and DDV-derived values of Λ in these regions of the observed clouds are generally between 25 cm^{-1} and 9 cm^{-1}. Similar exponential slopes are sometimes observed in snowfalls [e.g., *Matrosov et al.*, 2009]. It is not unusual to observe ice particle populations with such relatively low values of the exponential slope parameter in thick clouds too as shown by in situ aircraft sampling [e.g., *Heymsfield et al.*, 2008].

[37] It is puzzling that DDV-based retrievals were not good in the lower part of the 24 May cloud below about 7 km. DDV measurements there were around 0 (Figure 5d) although the DFR retrievals suggest the largest particles in this region. Some plausible explanation for this fact can be offered, however. As seen from Figures 3g and 3h, the observed Doppler velocities there were the highest. They reached 1.7–1.9 m s^{-1} (even if averaged for 0.5–1 h time periods). For the ground pressure it approximately corresponds to 1.15–1.3 m s^{-1}. Microphysical modeling studies of ice aggregate fall velocities, V_t [e.g., *Khvorostyanov and Curry*, 2002; *Mitchell and Heymsfield*, 2005], show that the power-law-like behavior of V_t – particle size relations breaks down for larger V_t values. V_t can actually decrease with size for very large particles due to changes in particle aerodynamic properties [*Mitchell and Heymsfield*, 2005, Figure 5]. As a result, negative DDV values are not out of question for larger ice hydrometeors, which exhibit very large absolute fall velocities.

[38] Overall, DFR-based estimates of the exponential PSD slope could be obtained for more cloud regions compared to DDV-based retrievals. One exception is the thin layer near the cloud base observed between about 22:00 and 23:00 UTC for the 7 May 2007 observational case. DFR values were less than 0.9 dB there, so the corresponding retrievals were not attempted. DDV-based retrievals, however, were available, though the corresponding values of Λ were close to the estimated above limit for this type of retrieval for this observational case.

[39] On average, for cloud parts where both types of retrievals are available in the approximate range 9 $cm^{-1} < \Lambda < 25$ cm^{-1}, the agreement between results of Λ estimates from DFR and DDV measurements is quite reasonable. This is rather encouraging because these retrievals use independent measurements. The mean relative bias (RB) and relative standard deviation (RSD) between Λ retrievals from DFR and DDV data (Λ_{DFR} and Λ_{DDV}, correspondingly) are about 26 and 45%, 14 and 49%, and 44 and 58% for the events of 7 May, 24 May, and 20 June 2007, respectively. The RB and RSD values were calculated for data points with continuously available retrievals (i.e., between about 5.5 and 8.5 km for the cloud observed on 7 May 2010, between 7 km and 10 km for the anvil cloud observed on 24 May 2010, and between 7 km and 9 km for the cloud observed on 20 June 2007) using the relations

$$RB = \left\langle 2(\Lambda_{DFR} - \Lambda_{DDV})(\Lambda_{DFR} + \Lambda_{DDV})^{-1} \right\rangle \times 100\%, \quad (9)$$

$$RSD = \left\langle 4(\Lambda_{DFR} - \Lambda_{DDV})^2(\Lambda_{DFR} + \Lambda_{DDV})^{-2} \right\rangle^{0.5} \times 100\%, \quad (10)$$

where angle brackets denote averaging.

[40] Changes in the horizontal airflow at different heights inside the cloud can influence the DDV retrievals when the radar beams are not exactly aligned, which was a suspected case for the event of 7 May 2007. While there is no unambiguous information to estimate the DDV bias changes inside the cloud because the antenna misalignment characteristics are not known, some assessments still can be made. To assess the influence of possible changes in airflow, DDV retrievals were also performed using the DDV bias values changed

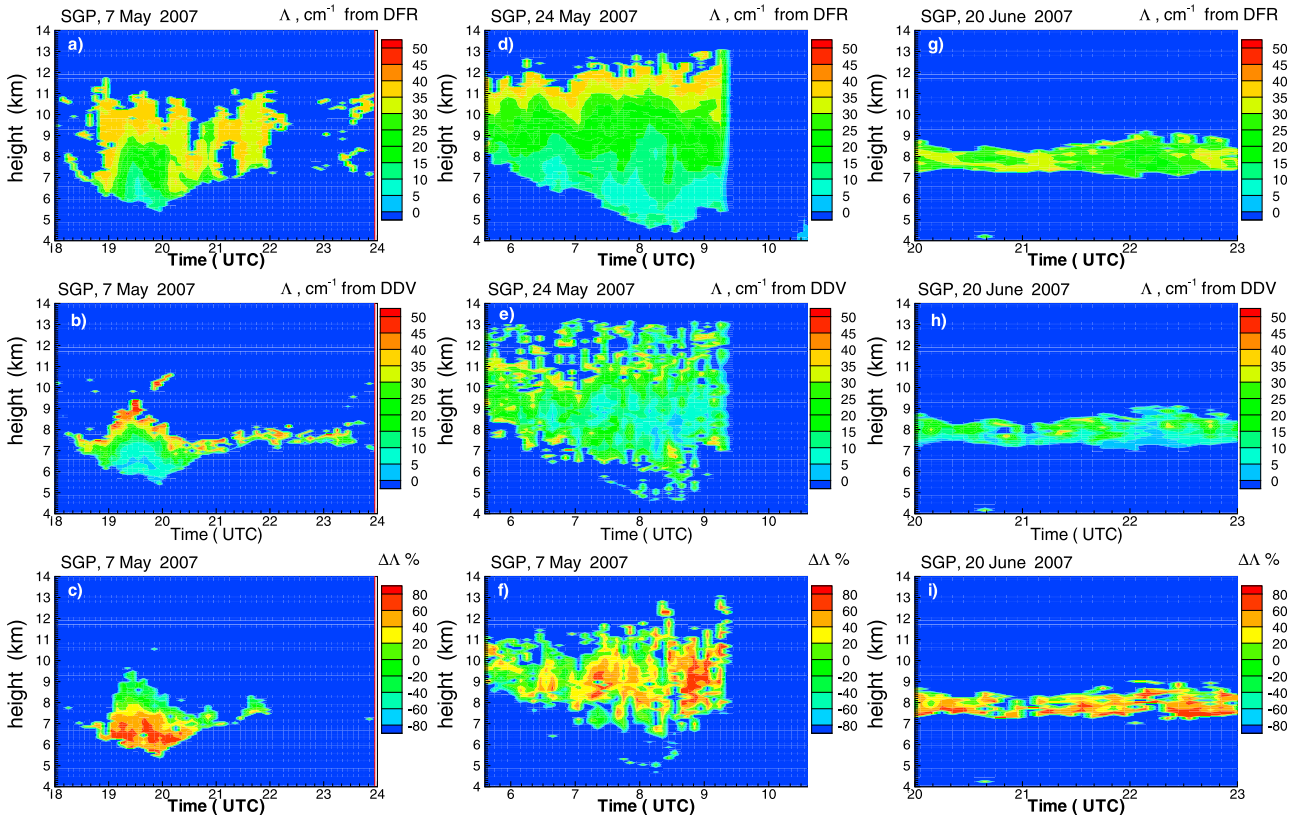

Figure 7. Time-height cross sections of (a, d, g) DFR-based retrievals, (b, e, h) DDV-based retrievals of the exponential slope of PSD, Λ, and (c, f, i) the relative difference of these retrievals $\Delta\Lambda = \Lambda(\mathrm{DFR}) - \Lambda(\mathrm{DDV})/\Lambda(\mathrm{DFR}) \times 100\%$. Observational cases of 7 May 2007 (Figures 7a, 7b, 7c), 24 May 2007 (Figures 7d, 7e, 7f), and 20 June 2007 (Figures 7g, 7h, 7i).

by 30% from the originally assumed value (i.e., -0.27 ± 0.08 m s^{-1}). These retrievals (not shown) resulted in RB and RSD of 15 and 41% (for the DDV bias -0.19 m s^{-1}) and 39 and 51% (for the DDV bias -0.35 m s^{-1}).

[41] Comparisons of dual-frequency radar retrievals with independent robust measurements from other remote sensors are not readily available. The use of optical instruments (e.g., lidars, IR interferometers) is limited because of the high optical density of thick ice clouds and also due to the fact that very large particles are often in the asymptotic scattering/absorption regime for optical wavelengths. Direct comparisons with simultaneous aircraft measurements were also unavailable. Uncertainties of PSD slope retrievals using the suggested approaches, however, can be estimated theoretically.

5. Estimates of Retrieval Uncertainties

[42] Uncertainties of retrieved values of Λ are determined by the DFR and DDV measurements errors and uncertainties in the model assumptions. The SD values in DFR and DDV measurements at the cloud top height levels after removing the mean bias could be assumed to be representative for the measurement noise. Figure 8a shows the relative errors $(\delta\Lambda/\Lambda)_{\mathrm{m}}$ in exponential slope retrievals due to these measurement errors assuming DFR and DDV measurement uncertainties of δDFR ≈ 0.9 dB and δDDV ≈ 0.03 m s^{-1}, correspondingly. For a given value of Λ, these errors were calculated from

$$(\delta\Lambda/\Lambda)_{\mathrm{m}} = 0.5[\Lambda(\mathrm{DFR} - \delta\mathrm{DFR}) - \Lambda(\mathrm{DFR} + \delta\mathrm{DFR})]\ \Lambda^{-1} \cdot (\text{for DFR-based retrievals}) \quad (11)$$

$$(\delta\Lambda/\Lambda)_{\mathrm{m}} = 0.5[\Lambda(\mathrm{DDV} - \delta\mathrm{DDV}) - \Lambda(\mathrm{DDV} + \delta\mathrm{DDV})]\ \Lambda^{-1} \cdot (\text{for DDV-based retrievals}). \quad (12)$$

In (11) and (12), Λ-DFR and Λ-DDV correspondences were calculated using the relations in Figure 2a for $r = 0.6$.

[43] It can be seen from Figure 8a that for larger values of Λ (i.e., for ice particle populations with smaller characteristic sizes), the retrieval errors due to measurement uncertainties rapidly increase because of the steepness of the Λ trends for smaller DFR and DDV values. These errors reach about 100% at $\Lambda \approx 45$ cm^{-1} (for DFR-based retrievals) and at $\Lambda \approx 35$ cm^{-1} (for DDV-based retrievals). For smaller PSD exponential slopes, the Λ(DFR) and Λ(DDV) curves flatten.

[44] Effects of mismatching measurement sample volumes due to differences in radar beam widths and range resolutions are a source of errors in DFR and DDV values used for retrievals. These effects contribute to the DFR and DDV standard deviations observed near the cloud top, where particles are generally small so that scattering is expected to be

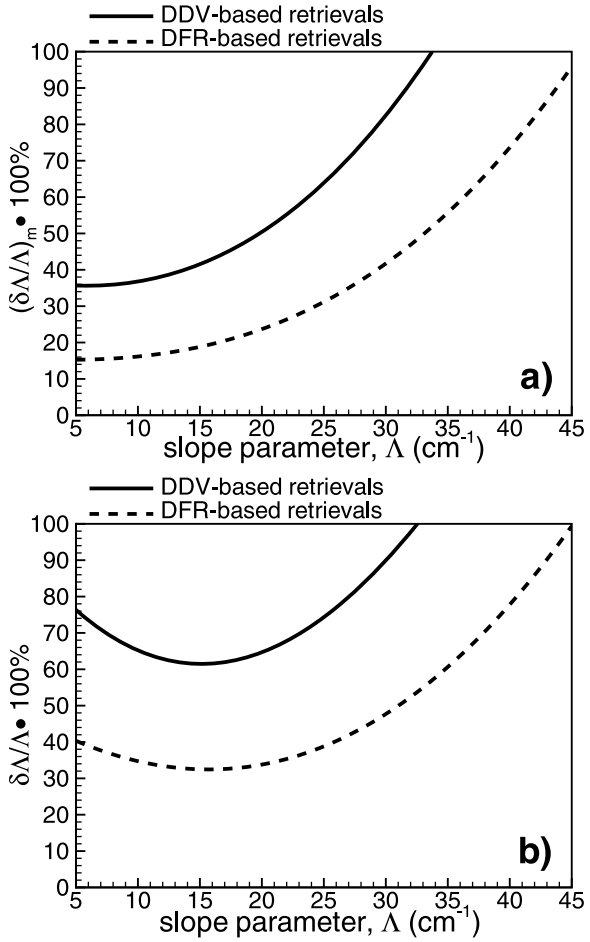

Figure 8. Relative errors of DFR- and DDV-based retrievals of the Λ parameter caused by (a) measurement uncertainties and (b) total relative retrieval errors due to measurement and assumption uncertainties.

in the Rayleigh regime for both frequencies. The beam widths of the MMCR and WACR result in about 30 and 50 m across the beam (for a typical height of 8 km) resolutions for these radars. Since horizontal winds at cloud levels are usually significant (Figure 6), time averaging resulting in sample overlapping alleviates the effects of these differences. While the beam width difference effect is difficult to quantify, *Hogan et al.* [2005], based on their measurements with vertically pointing radars, concluded that the beam mismatching effect is small if radar sample volume overlap is used. Note that for off-vertical measurements and smaller dwells, this effect can be more substantial [e.g., *Williams and Vivekanandan*, 2007].

[45] Noisier DFR and DDV values will result in higher retrieval uncertainties due to measurement errors. For example, assuming δDFR $\approx$ 1.2 dB and δDDV $\approx$ 0.05 m s^{-1} will result in the minimal relative errors shown in Figure 8a increased by factors of about 1.35 and 2 for DFR- and DDV-based retrievals, correspondingly. The increase in measurement noise in DFR and DDV estimates could be caused by a variety of factors including stronger effects due to beam misalignments and sample volume mismatched, and thus it is important to monitor the variability of these parameters near the cloud top.

[46] Judging on the retrieval accuracies due to measurement noise, which were estimated for these observations, DFR-based retrievals of Λ are generally more accurate compared to the DDV-based retrievals. Figure 8 shows that for the same value of the exponential slope Λ, the corresponding difference in estimated retrieval errors using these two dual-frequency remote sensing approaches is about a factor of 2. The better accuracies from DFR measurements can be explained, in part, by the fact that non-Rayleigh scattering effects are generally more strongly manifested in the reflectivity ratios. The Doppler velocity differences, on the other hand, are generally less pronounced, in part because the terminal fall velocities of larger ice particles depend on particle size rather weakly due to a relatively low value of the exponent b in (7).

[47] Besides measurement errors, other significant sources of retrieval uncertainties are uncertainties in model assumptions. These sources include the variability of the Λ-DFR and Λ-DDV relations caused by uncertainties in particle aspect ratios, densities, PSD types caused by the variability of the parameter μ, and (specifically for the Λ-DDV relation) by the uncertainty in the assumed particle terminal fall velocity–size relation. The model uncertainties increase total errors of the exponential slope retrievals, and they need to be estimated.

[48] The errors due to the variability of particle aspect ratios, $(\delta\Lambda/\Lambda)_r$ at a given Λ level, were estimated as

$$(\delta\Lambda/\Lambda)_r = |\Lambda_{0.6}(\mathrm{DFR}) - \Lambda_{0.8}(\mathrm{DFR})|/\Lambda_{0.6}(\mathrm{DFR}) \cdot (\text{for DFR-based retrievals}), \quad (13)$$

$$(\delta\Lambda/\Lambda)_r = |\Lambda_{0.6}(\mathrm{DDV}) - \Lambda_{0.8}(\mathrm{DDV})|/\Lambda_{0.6}(\mathrm{DDV}) \cdot (\text{for DDV-based retrievals}), \quad (14)$$

where the correspondences between $\Lambda_{0.6}$ (or $\Lambda_{0.8}$) and DFR and DDV values are determined from the Λ-DFR and Λ-DDV relations for r = 0.6 (or r = 0.8) in Figure 2a. As mentioned in section 3, PSD shape factor μ changes and particle bulk density variations affect the dual-frequency radar parameters relatively little compared to the particle shape effects.

[49] The DDV-based retrieval errors have an additional contribution from uncertainties in the coefficients of fall velocity–size relations (7). As discussed in section 2, a 20% change in the coefficient a in (7) provides a proxy for the variability in these relations. A corresponding error contribution could be estimated as

$$(\delta\Lambda/\Lambda)_v = 0.5|\Lambda_{0.55}(\mathrm{DDV}) - \Lambda_{0.85}(\mathrm{DDV})|/\Lambda_{0.7}(\mathrm{DDV}), \quad (15)$$

where $\Lambda_{0.55}$, $\Lambda_{0.85}$ and $\Lambda_{0.7}$ are calculated using the Λ-DDV relations for the coefficients a = 0.55, 0.85, and 0.7, respectively (note that the relations for a = 0.55 and 0.85 are not shown in Figure 2).

[50] Assuming that different error contributions are independent, the total retrievals errors can be estimated as

$$(\delta\Lambda/\Lambda)^2 = (\delta\Lambda/\Lambda)_m^2 + (\delta\Lambda/\Lambda)_r^2 (\text{for DFR-based retrievals}), \quad (16)$$

$$(\delta\Lambda/\Lambda)^2 = (\delta\Lambda/\Lambda)_m^2 + (\delta\Lambda/\Lambda)_r^2 + (\delta\Lambda/\Lambda)_v^2 \cdot (\text{for DFR-based retrievals}). \quad (17)$$

These estimates are shown in Figure 8b. Contributions from variations in μ and particle density change results insignificantly.

[51] Comparisons of Figure 8a and Figure 8b show that the total retrievals errors are noticeably larger than those which are only due to measurement uncertainty. This is especially true for $\Lambda < 25$ cm^{-1}. For smaller values of Λ, errors even increase as the slope parameter decreases. This is caused by relatively larger model uncertainties in relating dual-frequency radar parameters and Λ for $\Lambda < 9$ cm^{-1}. The smallest retrieval errors are expected for slope parameter values between about 9 cm^{-1} and 25 cm^{-1}. As noted above, for larger differential Doppler velocity measurement noise total expected DDV-based retrieval errors could be noticeably higher than those in Figure 8.

[52] As mentioned previously, comparisons of the DFR- and DDV-based Λ retrievals for cloud regions where both types of estimates are continuously available (Figure 7) indicated relative biases of ~14–44% and relative standard deviations of ~45–58%. These RSD values are of the order of the retrieval error from DFR and are smaller than the estimated error of retrievals from DDV. This indicates a general consistency of the retrievals.

[53] While the base model assumptions made in this study and the corresponding retrievals appear to be reasonable, there was no way to confirm them with direct in situ measurements. There are, however, some additional consistency checks that can be conducted. One such test is to use retrievals of Λ from dual-frequency approaches and to calculate the absolute Doppler velocities and then compare them to the observed values. The best agreement between Λ retrieved from DFR and DDV measurements for the event of 7 May 2007 was observed between heights of 7 and 7.5 km during the time interval between 19:20 and 20:00 UTC (see Figure 7). The corresponding Λ values were in an interval of about 18–22 cm^{-1} from both types of retrievals. The expected retrieval errors for this interval of Λ are the smallest (see Figure 8). The K_a-band Doppler velocities were calculated using these Λ values and relations (5) and (7) (with $a = 0.7$ and $b = 0.25$) for the time-height cloud area mentioned above. The time-averaged value of V_D in this area was ~0.77 m s^{-1} near the ground and ~1.12 m s^{-1} after scaling it to the height of 7.25 km using the air density correction. This value is in good agreement with the observed mean value of V_D, which was 1.1 m s^{-1} (see Figure 3c). Note that the vertical air motion contribution in the observed value of V_D is expected to be small due to significant time averaging (i.e., ~40 min for this example). A similar absolute Doppler velocity consistency (~1.25 m s^{-1} after scaling the height of observations) was obtained with the best agreement Λ data (18–22 cm^{-1}) at a 9 km height between 07:30 and 09:20 UTC (i.e., when variations in the observed Doppler velocity and retrieved PSD slope data were minimal) for the anvil cloud case from 24 May 2007.

[54] For the observational case of 20 June 2007, a consistency between estimated and observed V_D is also generally present for the areas where both retrievals yielded similar results. While not a robust verification, these consistency checks indicate the general appropriateness of the chosen V_t-D relation. Consistency checks for absolute reflectivities were not possible because Z_e values depend on the intercept parameter N_o (besides being dependent on Λ), which is not retrievable with the dual-frequency approaches considered in this study.

[55] Since for the exponential distributions, which were shown to adequately describe PSD moments in high reflectivity ice clouds [*Heymsfield et al.*, 2008], the slope parameter Λ is inversely proportional to the median volume particle size D_0 (equation (4)). Since $|\partial D_0/\partial\Lambda| = D_0/\Lambda$, the relative error estimates of Λ presented above also approximately correspond to retrieval errors of this characteristic size. The retrieval results given in terms of Λ can be converted to D_0 using the expression $D_0 \approx 3.67/\Lambda$. The 9 cm^{-1} – 25 cm^{-1} Λ interval of the smallest relative errors correspond to the D_0 interval between about 1.4 and 4.0 mm. In addition to D_0, some other characteristic sizes are often being used to describe PSDs (e.g., the effective radius R_{eff} or the effective diameter D_{eff}, which are proportional to the ratio of the PSD volume at bulk ice density to the total projected area). Uncertainties in retrieving D_{eff} from dual-frequency radar approaches depend on density and habit assumptions stronger compared to Λ and D_0. As a result, potential retrieval errors for D_{eff} could be significantly larger than those for D_0. As suggested by *Matrosov et al.* [2003], D_{eff} could be approximately estimated from D_0 using two coefficients which might have uncertainties of about 40%. These coefficients depend on parameters of the mass – size and mass – projected area – size relations. If the independence of error contributions is assumed (i.e., the contributions from uncertainties in the aforementioned coefficients and in D_0 estimates), the total smallest estimation error for D_{eff} could be as large as about 85 (from DDV) and 65% (from DFR) compared to about 65 and 35% for Λ (and also for D_0) as shown in Figure 8.

[56] The radar-based methods are better suited for estimating PSD size parameters, which are related to particle physical dimensions (i.e., D_0 and Λ), than size parameters that are related to cloud optical properties (as D_{eff} or R_{eff}, which define correspondence between PSD bulk mass and extinction). The approaches discussed in this study are aimed at particle physical dimension parameters retrievals. Effective sizes retrievals present a greater challenge and warrant a separate research utilizing particular mass – size and mass – projected area – size relations.

6. Discussion and Conclusions

[57] Modeling and ground-based radar measurements from vertically pointing K_a- and W-band ARM cloud radars were used to evaluate the applicability and potential accuracy of dual-frequency remote sensing approaches to infer aggregate particle size information in thick ice clouds. Two independent methods (one traditional method based on dual-frequency reflectivity ratio (DFR) measurements and the other novel method based on differential Doppler velocity (DDV) measurements) for retrievals of the exponential slope Λ of particle size distributions were tested. This slope is directly related to the median volume particle size D_0 ($\Lambda \approx 3.67/D_0$) which characterizes the PSD. Estimates of the characteristic size using the dual-frequency approaches show relatively little sensitivity to the PSD type. The DDV approach has an advantage over the single-frequency Doppler radar techniques for sizing larger ice particles due to the fact that it is immune to the vertical air motions so it

can be used for retrievals with higher temporal resolutions. A precise vertical alignment of radar beams is important as the "leak" of horizontal winds into vertical Doppler measurements is a limiting factor for DDV-based retrievals.

[58] DFR measurements need to be constrained near the cloud top where particles are small and dual-frequency reflectivity effects are not present. Constraining is needed due to uncertainties in radar absolute calibrations and because attenuation in the atmospheric layer below the cloud base is wavelength dependent and may vary in time. Since DDV measurements are not affected by attenuation and absolute calibration uncertainties, they generally do not need to be constrained at the cloud top. However, for the experimental setting of the radars during some analyzed observations, a possible small pointing mismatch could have resulted in a DDV bias, which was corrected by a cloud top constraint. The variability of DFR and DDV measurements near the cloud top where particles are generally small and no wavelength-dependent differences in the scattering regime are expected was assumed to be representative of the dual-wavelength parameter measurement noise. This noise is affected by effects of the radar beam width mismatch and range resolution differences. Time averaging and vertical data interpolating to the common vertical resolution were used to mitigate these effects.

[59] The DFR- and DDV-based approaches were applied to observations of thick ice clouds. The retrieval results revealed a general consistency of DFR- and DDV-based estimates of the PSD slope, although the later estimates were generally noisier. In cloud regions where both types of retrievals were continuously available (generally for $9\ \mathrm{cm}^{-1} < \Lambda < 25\ \mathrm{cm}^{-1}$), the relative bias and the relative standard deviation of estimated values of Λ were about 14–44% and 45–58%, respectively. These discrepancies were within the estimated retrieval errors.

[60] The retrieval errors were assessed by taking into account measurement noise and uncertainties in different model assumptions including assumptions about the PSD types, ice particle shapes, and densities. The estimated retrieval errors for the DFR approach were about 40% for Λ values in a range between approximately $9\ \mathrm{cm}^{-1}$ and $25\ \mathrm{cm}^{-1}$ assuming an about 0.9 dB uncertainty in DFR values. The retrievals of higher values of Λ become progressively less certain due to decreasing non-Rayleigh scattering effects. Retrieval errors also increase for PSDs with lower values of Λ, which is due to an increase in model uncertainties for larger particle populations and to the fact that dual-frequency dependencies generally flatten as Λ decreases. Another source of retrieval uncertainties for small size parameters Λ is the higher dependence of dual-frequency parameters on particle model for large aggregates. This can make retrievals not very practical for $\Lambda < 8$–$9\ \mathrm{cm}^{-1}$.

[61] Estimated errors for DDV-based retrievals are generally higher than those for DFR-based retrievals by about a factor of 2 for the common assumption about model and measurement uncertainties. Since microphysical modeling studies indicate that fall velocities for very large aggregate particles deviate from the power law approximation and can even decrease with particle size, the DDV-based approach also has an applicability limitation for such particle populations. An anvil cloud case study indicated that such limitation can be already present when typical averaged Doppler velocities are in excess of about 1.6–1.8 m s^{-1} (at about 6 km height). Expected DDV-based retrieval errors can further increase with noisier DDV values.

[62] While retrievals from Doppler velocity differences are potentially less certain and could be available for a smaller Λ interval compared to DFR retrievals, the DDV approach may have some advantages in certain observational situations when applications of the DFR approach may be limited. Such situations may include observations of ice regions in precipitating clouds when strong attenuation in liquid and melting hydrometeors beneath will prevent radar signals from reaching cloud tops with small particle populations. As a result, a cloud top constraint for DFR measurements will not be available. DDV measurements, on the other hand, do not require such a constraint given that radar beams are precisely aligned in the vertical. Another example, when the DFR approach could be very limited, is observations of clouds with a substantial amount of supercooled water, which could mask the DFR signals due to differential attenuation but not DDV signals which are unaffected by attenuation. A detailed consideration of dual-frequency radar approaches for such observational situations is beyond the scope of this study.

[63] While the scope of this study is limited to assessing the feasibility of the dual-wavelength radar approaches using theoretical considerations and case observations, more experimental studies in thick ice clouds and snowfall with precisely aligned radar beams are needed to better understand the accuracy of such approaches. Possible theoretical advancements may include considerations of improved particle fall velocity size relations and aggregate models. Accounting for possible correlations between different model assumptions (e.g., fall velocity-size and mass-size relations) may refine retrieval uncertainty estimates. Possible observational enhancements can include the use of radar polarization measurements to independently assess predominant particle shapes (aspect ratios) so the retrieval uncertainty contribution due to particle habit variability may be reduced. Achieving the best possible spatial and temporal matching of observations is an important factor for future studies using dual-wavelength radar approaches.

[64] **Acknowledgment.** Data were obtained from the Atmospheric Radiation Measurement Program sponsored by the U.S. Department of Energy, Office of Science, Office of Biological and Environmental Sciences Division.

References

Barber, P., and C. Yeh (1975), Scattering of electromagnetic waves by arbitrarily shaped dielectric bodies, *Appl. Opt.*, *14*, 2864–2872.

Brandes, E. A., K. Ikeda, G. Thompson, and M. Schönhuber (2008), Aggregate terminal velocity/temperature relations, *J. Appl. Meteorol. Climatol.*, *12*, 410–414.

Brown, P. R. A., and P. N. Francis (1995), Improved measurements of ice water content in cirrus using a total water probe, *J. Atmos. Oceanic Technol.*, *12*, 410–414, doi:10.1175/1520-0426(1995)012<0410:IMOTIW>2.0.CO;2.

Comstock, J. M., et al. (2007), An intercomparison of microphysical retrieval algorithms for upper tropospheric ice clouds, *Bull. Am. Meteorol. Soc.*, *88*, 191–204, doi:10.1175/BAMS-88-2-191.

Donovan, D. P., and C. A. P. van Lammeren (2001), Cloud effective particle size and water content profile retrievals using combined lidar and radar observations: 1. Theory and examples, *J. Geophys. Res.*, *106*, 27,425–27,448, doi:10.1029/2001JD900243.

Doviak, R. J., and D. S. Zrnic (1993), *Doppler Radar and Weather Observations*, 562 pp., Academic, San Diego, Calif.

Heymsfield, A. J., P. Field, and A. Bansemer (2008), Exponential size distributions for snow, *J. Atmos. Sci.*, *65*, 4017–4031, doi:10.1175/2008JAS2583.1.

Hogan, R. J., A. J. Illingworth, and H. Sauvageot (2000), Measuring crystal size in cirrus using 35- and 94-GHz radars, *J. Atmos. Oceanic Technol.*, *17*, 27–37, doi:10.1175/1520-0426(2000)017<0027:MCSICU>2.0.CO;2.

Hogan, R. J., N. Gaussiat, and A. J. Illingworth (2005), Stratocumulus liquid water content from dual-wavelength radar, *J. Atmos. Oceanic Technol.*, *22*, 1207–1218, doi:10.1175/JTECH1768.1.

Khvorostyanov, V. I., and J. A. Curry (2002), Terminal velocities of droplets and crystals: Power laws with continuous parameters over size spectrum, *J. Atmos. Sci.*, *59*, 1872–1884, doi:10.1175/1520-0469(2002)059<1872:TVODAC>2.0.CO;2.

Korolev, A., and G. Isaac (2003), Roundness and aspect ratio of particles in ice clouds, *J. Atmos. Sci.*, *60*, 1795–1808, doi:10.1175/1520-0469(2003)060<1795:RAAROP>2.0.CO;2.

Liao, L., R. Meneghini, L. Tian, and G. M. Heymsfield (2008), Retrieval of snow and rain from combined X- and W-band airborne radar measurements, *IEEE Trans. Geosci. Remote Sens.*, *46*, 1514–1524, doi:10.1109/TGRS.2008.916079.

Lumb, F. E. (1961), Relation between the terminal velocity and dimensions of snowflake, *Meteorol. Mag.*, *90*, 344–347.

Mace, G. G., T. P. Ackerman, P. Minnis, and D. F. Young (1998), Cirrus layer microphysical properties derived from surface-based millimeter radar and infrared interferometer, *J. Geophys. Res.*, *103*, 23,207–23,216.

Mace, G. G., A. J. Heymsfield, and M. R. Poellot (2002), On retrieving the microphysical properties of cirrus clouds using the moments of the millimeter-wavelength Doppler spectrum, *J. Geophys. Res.*, *107*(D24), 4815, doi:10.1029/2001JD001308.

Marshall, J. S., and W. Hitschfeld (1953), Interpretation of the fluctuating echo from randomly distributed scatterers: Part 1, *Can. J. Phys.*, *31*, 962–994, doi:10.1139/p53-084.

Matrosov, S. Y. (1993), Possibilities of cirrus particle sizing from dual-frequency radar measurements, *J. Geophys. Res.*, *98*, 20,675–20,683, doi:10.1029/93JD02335.

Matrosov, S. Y. (2007), Modeling backscatter properties of snowfall at millimeter wavelengths, *J. Atmos. Sci.*, *64*, 1727–1736, doi:10.1175/JAS3904.1.

Matrosov, S. Y. (2009), Simultaneous estimates of cloud and rainfall parameters in the atmospheric vertical column above the Atmospheric Radiation Program southern Great Plains site, *J. Geophys. Res.*, *114*, D22201, doi:10.1029/2009JD012004.

Matrosov, S. Y., T. Uttal, J. B. Snider, and R. A. Kropfli (1992), Estimation of ice cloud parameters from ground-based infrared radiometer and radar measurements, *J. Geophys. Res.*, *97*, 11,567–11,574.

Matrosov, S. Y., A. V. Korolev, and A. J. Heymsfield (2002), Profiling cloud ice mass and particle characteristic size from Doppler radar measurements, *J. Atmos. Oceanic Technol.*, *19*, 1003–1018, doi:10.1175/1520-0426(2002)019<1003:PCIMAP>2.0.CO;2.

Matrosov, S. Y., M. D. Shupe, A. J. Heymsfield, and P. Zuidema (2003), Ice cloud optical thickness and extinction estimates from radar measurements, *J. Appl. Meteorol.*, *42*, 1584–1597, doi:10.1175/1520-0450(2003)042<1584:ICOTAE>2.0.CO;2.

Matrosov, S. Y., A. J. Heymsfield, and Z. Wang (2005a), Dual-frequency radar ratio of non-spherical atmospheric hydrometeors, *Geophys. Res. Lett.*, *32*, L13816, doi:10.1029/2005GL023210.

Matrosov, S. Y., R. F. Reinking, and A. V. Djalalova (2005b), Inferring fall attitudes of pristine dendritic crystals from polarimetric radar data, *J. Atmos. Sci.*, *62*, 241–250, doi:10.1175/JAS-3356.1.

Matrosov, S. Y., C. Campbell, D. Kingsmill, and E. Sukovich (2009), Assessing snowfall rates from X-band radar reflectivity measurements, *J. Atmos. Oceanic Technol.*, *26*, 2324–2339, doi:10.1175/2009JTECHA1238.1.

Mazin, I. P. (Ed.) (1989), *Clouds and the Cloudy Atmosphere*, 648 pp., Gidrometeoizdat, Leningrad, Russia.

Mitchell, D. L., and A. J. Heymsfield (2005), Refinements in the treatment of ice particle terminal velocities, highlighting aggregates, *J. Atmos. Sci.*, *62*, 1637–1644, doi:10.1175/JAS3413.1.

Okamoto, H., S. Iwasaki, M. Yasui, H. Horie, H. Kuroiwa, and H. Kumagai (2003), An algorithm for retrieval of cloud microphysics using 95-GHz cloud radar and lidar, *J. Geophys. Res.*, *108*(D7), 4226, doi:10.1029/2001JD001225.

Pruppacher, H. R., and J. D. Klett (1978), *Microphysics of Clouds and Precipitation*, 714 pp., D. Reidel, Dordrecht, Netherlands.

Reinking, R. F., S. Y. Matrosov, R. A. Kropfli, and B. W. Bartram (2002), Evaluation of a slant 45° quasi-linear radar polarization for distinguishing drizzle droplets, pristine ice crystals, and less regular ice particles, *J. Atmos. Oceanic Technol.*, *19*, 296–321, doi:10.1175/1520-0426-19.3.296.

Sekelsky, S. M., W. L. Ecklund, J. M. Firda, K. S. Gage, and R. E. McIntosh (1999), Particle size estimations in ice-phase clouds using multifrequency radar reflectivity measurements at 95, 33, and 2.8 GHz, *J. Appl. Meteorol.*, *38*, 5–28, doi:10.1175/1520-0450(1999)038<0005:PSEIIP>2.0.CO;2.

Tian, L., G. M. Heymsfield, L. Li, and R. C. Srivastava (2007), Properties of light stratiform rain derived from 10 and 94-GHz airborne Doppler radar, *J. Geophys. Res.*, *112*, D11211, doi:10.1029/2006JD008144.

Wang, Z., and K. Sassen (2002), Cirrus cloud microphysical property retrieval using lidar and radar measurements: Part I. Algorithm description and comparison with in situ data, *J. Appl. Meteorol.*, *41*, 218–229, doi:10.1175/1520-0450(2002)041<0218:CCMPRU>2.0.CO;2.

Wang, Z., G. M. Heymsfield, L. Li, and A. J. Heymsfield (2005), Retrieving optically thick ice cloud microphysical properties by using dual-wavelength radar measurements, *J. Geophys. Res.*, *110*, D19201, doi:10.1029/2005JD005969.

Williams, J. K., and J. Vivekanandan (2007), Sources of error in dual-wavelength radar remote sensing of cloud liquid water content, *J. Atmos. Oceanic Technol.*, *24*, 1317–1336, doi:10.1175/JTECH2042.1.

S. Y. Matrosov, Earth System Research Laboratory, NOAA, R/PSD2, 325 Broadway, Boulder, CO 80305, USA. (sergey.matrosov@noaa.gov)